

LETTER TO THE EDITOR

# Signatures of rocky planet engulfment in HAT-P-4<sup>★,★★</sup>

## Implications for chemical tagging studies

C. Saffe<sup>1,2,4</sup>, E. Jofré<sup>3,4</sup>, E. Martioli<sup>5</sup>, M. Flores<sup>1,2,4</sup>, R. Petrucci<sup>3,4</sup>, and M. Jaque Arancibia<sup>1,4</sup>

<sup>1</sup> Instituto de Ciencias Astronómicas, de la Tierra y del Espacio (ICATE-CONICET), C.C 467, 5400 San Juan, Argentina  
e-mail: csaffe@conicet.gov.ar

<sup>2</sup> Universidad Nacional de San Juan (UNSJ), Facultad de Ciencias Exactas, Físicas y Naturales (FCEF), San Juan, Argentina

<sup>3</sup> Observatorio Astronómico de Córdoba (OAC), Laprida 854, X5000BGR, Córdoba, Argentina  
e-mail: emiliano@oac.unc.edu.ar

<sup>4</sup> Consejo Nacional de Investigaciones Científicas y Técnicas (CONICET), Argentina

<sup>5</sup> Laboratório Nacional de Astrofísica (LNA/MCTI), rua Estados Unidos 154, Itajubá, MG, Brazil  
e-mail: emartioli@lna.br

Received 23 June 2017 / Accepted 6 July 2017

### ABSTRACT

**Aims.** We aim to explore the possible chemical signature of planet formation in the binary system HAT-P-4 by studying the trends of abundance vs. condensation temperature  $T_c$ . The star HAT-P-4 hosts a planet detected by transits, while its stellar companion does not have any detected planet. We also study the lithium content, which might shed light on the problem of Li depletion in exoplanet host stars.

**Methods.** We derived for the first time both stellar parameters and high-precision chemical abundances by applying a line-by-line full differential approach. The stellar parameters were determined by imposing ionization and excitation equilibrium of Fe lines, with an updated version of the FUNDPAR program, together with ATLAS9 model atmospheres and the MOOG code. We derived detailed abundances of different species with equivalent widths and spectral synthesis with the MOOG program.

**Results.** The exoplanet host star HAT-P-4 is found to be  $\sim 0.1$  dex more metal rich than its companion, which is one of the highest differences in metallicity observed in similar systems. This could have important implications for chemical tagging studies. We rule out a possible peculiar composition for each star, such as is the case for  $\lambda$  Boötis and  $\delta$  Scuti, and neither is this binary a blue straggler. The star HAT-P-4 is enhanced in refractory elements relative to volatile when compared to its stellar companion. Notably, the Li abundance in HAT-P-4 is greater than that of its companion by  $\sim 0.3$  dex, which is contrary to the model that explains the Li depletion by the presence of planets. We propose a scenario where at the time of planet formation, the star HAT-P-4 locked the inner refractory material in planetesimals and rocky planets, and formed the outer gas giant planet at a greater distance. The refractories were then accreted onto the star, possibly as a result of the migration of the giant planet. This explains the higher metallicity, the higher Li content, and the negative  $T_c$  trend we detected. A similar scenario was recently proposed for the solar-twin star HIP 68468, which is in some aspects similar to HAT-P-4. We estimate a mass of at least  $M_{\text{rock}} \sim 10 M_{\oplus}$  locked in refractory material in order to reproduce the observed  $T_c$  trends and metallicity.

**Key words.** stars: abundances – planetary systems – binaries: general – stars: individual: TYC 2569-744-1 – stars: individual: HAT-P-4

## 1. Introduction

The detection of a possible chemical signature of planet formation in the photospheres of planet host stars is a challenge for current studies. Several authors have attempted to detect this signature by studying the condensation temperature ( $T_c$ ) trend in planet host stars (e.g., Gonzalez 1997; Smith et al. 2001; Gratton et al. 2001). In particular, Meléndez et al. (2009)

showed that the atmosphere of the Sun is deficient in refractory<sup>1</sup> elements when compared to the average abundances of 11 solar twins, also showing a clear  $T_c$  trend. They proposed that the missing refractories are probably locked in terrestrial planets and rocky material that orbits the Sun. This idea was then supported by Ramírez et al. (2009), who studied a sample of 64 solar twins and analogs with and without planets. On the other hand, other authors suggest that the  $T_c$  trends depend on the galactic chemical evolution (GCE), the stellar age, or probably the galactic birth place of the stars (e.g., Adibekyan et al. 2014, 2016), which competes with the proposed chemical signature of planet formation (e.g. González Hernández et al. 2013).

Most multiple and binary stars are believed to have formed coevally from a common molecular cloud. Wide binaries are particularly valuable because both components can be presumed to have the same age and initial composition, greatly diminishing

\* Based on observations obtained at the Gemini Observatory, which is operated by the Association of Universities for Research in Astronomy, Inc., under a cooperative agreement with the NSF on behalf of the Gemini partnership: the National Science Foundation (US), the National Research Council (Canada), CONICYT (Chile), Min. de Ciencia y Tecnología (Argentina), and Ministério da Ciência, Tecnologia e Inovação (Brazil).

\*\* The average abundances, the line-by-line data and the reduced spectra (FITS files) are only available at the CDS via anonymous ftp to [cdsarc.u-strasbg.fr](http://cdsarc.u-strasbg.fr) (130.79.128.5) or via <http://cdsarc.u-strasbg.fr/viz-bin/qcat?J/A+A/604/L4>

<sup>1</sup> Refractory and volatile species are those with  $T_c > 900$  K and  $T_c < 900$  K.

the mentioned age and GCE effects. Several studies have shown that there may be small differences in the chemical composition of their components, possibly due to the planet formation process (Gratton et al. 2001; Desidera et al. 2004, 2006). The similarity between the two components of a binary system enabled achieving a higher precision in a differential study (e.g., Saffe et al. 2015, 2016). To date, more than 2700 planetary systems have been reported<sup>2</sup>, but only a handful of these systems are binaries with similar components. Three of these remarkable systems were studied in detail: 16 Cyg, HAT-P-1, and HD 80606 (Laws & Gonzalez 2001; Ramírez et al. 2011; Schuler et al. 2011; Tucci Maia et al. 2014; Liu et al. 2014; Saffe et al. 2015). There are also binary systems in which circumstellar planets orbit both stars of the system (e.g., Mack et al. 2014). These studies show that a  $T_c$  trend is probably present between the stars of 16 Cyg, but not in the cases of HAT-P-1 or HD 80606. Notably, the binary system  $\zeta^2$  Ret (where one component is orbited by a dust disk with no planet detected) also shows a  $T_c$  trend between their stars, supporting the chemical signature of planet formation (Saffe et al. 2016). This clearly shows that additional systems need to be studied through detailed abundance analyses in order to reach more significant conclusions.

As a result of the planetary transit survey HATNet, Kovács et al. (2007) discovered a giant planet of  $0.68 M_{\text{Jup}}$  orbiting the star HAT-P-4 (=BD +36 2593) at a distance of 0.04 AU. They estimated a density of  $0.41 \text{ g cm}^{-3}$ , which is one of the lowest-density hot Jupiters known. Then, Mugrauer et al. (2014) showed that HAT-P-4 forms a wide binary system separated by 91.8 arcsec from its companion (TYC 2569-744-1, hereafter component B), and they also showed that both stars present very similar spectra (G0V + G2V). The estimated separation is 28 446 AU, which was considered by Mugrauer et al. (2014) as a true binary system based on their common proper motion and similar radial velocity. To date, there is no planet detected around the B star, which is also included in the field G191 (FOV =  $8 \times 8$  deg) of the HATNet survey (Kovács et al. 2007). As we show in the next sections, the stellar parameters of both stars are very similar, making this system an ideal case to study the possible chemical signature of planet formation.

Different authors have shown a possible excess of Li depletion in stars with planets compared to stars without planets (King et al. 1997; Israelian et al. 2004, 2009; Delgado-Mena et al. 2014; Gonzalez 2014, 2015). The Li depletion was first attributed to the presence of planets, which might possibly increase the angular momentum of the star (e.g., during planet migration) and increase its convective mixing (Israelian et al. 2009). On the other hand, some works showed that the Li depletion is related to a bias in age, mass, and metallicity and is not due to the presence of planets or the planet formation process (Luck & Heiter 2006; Baumann et al. 2010; Ramírez et al. 2012; Carlos et al. 2016). The study of similar stars in binary systems can help understand the origin of Li depletion. In the 16 Cyg binary system, the B component hosts a planet of  $1.5 M_{\text{Jup}}$  (Cochran et al. 1997) and presents a Li content that is about four times lower than that of the A star (King et al. 1997), which supports the model of Li depletion by the presence of planets. However, Ramírez et al. (2011) showed that the slightly different masses of stars A and B could explain their different Li contents, that is, 16 Cyg can in principle support both scenarios. Notably, HAT-P-4 is in some way complementary to 16 Cyg: in this case, the planet host star presents the higher Li content, which is contrary to the model of Li depletion

due to the presence of planets. Then, it is worthwhile exploring both the  $T_c$  trends and the Li depletion in this remarkable system.

## 2. Observations and data reduction

Observations of HAT-P-4 binary system were acquired through the Gemini Remote Access to CFHT ESPaDOnS Spectrograph (GRACES). This device takes advantage of the high-resolution ESPaDOnS<sup>3</sup> spectrograph, located at the Canada-France-Hawaii Telescope (CFHT) and fed by an optical fiber connected to the 8.1 m Gemini North telescope at Maunakea, Hawaii. We used the 1-fiber object-only observing mode, which provides an average resolving power of  $\sim 67\,500$  between 4500 and 8500 Å<sup>4</sup>. The stellar spectra were obtained under a fast-turnaround (FT) observing mode requested to the Gemini Observatory (program ID: GN-2016A-FT-25, PI: C. Saffe). The observations were taken on June 3, 2016, with the B star observed immediately after the A star, using the same spectrograph configuration for both stars. The exposure times were  $2 \times 17$  min on each target, obtaining a final signal-to-noise ratio (S/N) of  $\sim 400$  measured at  $\sim 6000$  Å in the combined spectra. The final spectral coverage is 4050–10 000 Å. The Moon was also observed with the same spectrograph setup, achieving a similar S/N to acquire the solar spectrum as initial reference. GRACES spectra were reduced using the code OPERA<sup>5</sup> (Martioli et al. 2012). More recent documentation on OPERA can be found at the ESPECTRO project webpage<sup>6</sup>.

## 3. Stellar parameters and abundance analysis

Fundamental parameters ( $T_{\text{eff}}$ ,  $\log g$ , [Fe/H], and  $v_{\text{turb}}$ ) were derived following a similar procedure as in our previous work (Saffe et al. 2015, 2016). We measured the equivalent widths (EW) of the Fe I and Fe II lines using the IRAF task *splot*, and then continued with other chemical species. Both the lines list and relevant laboratory data were taken from the literature (Liu et al. 2014; Meléndez et al. 2014; Bedell et al. 2014). We imposed an excitation and ionization balance of Fe lines using the differential version of the FUNDPAR program (Saffe 2011; Saffe et al. 2015). This code made use of ATLAS9 model atmospheres (Kurucz 1993) together with the 2014 version of the MOOG program (Snedden 1973). Stellar parameters were determined using the Sun as reference, that is, (A–Sun) and (B–Sun), by adopting (5777 K, 4.44 dex, 0.00 dex,  $0.91 \text{ km s}^{-1}$ ) for the Sun<sup>7</sup>. Then, we recalculated the parameters using the A star as reference, that is, (B–A), by adopting for the A star the parameters derived for the case (A–Sun) (see Table 1). The errors in the stellar parameters were derived following the procedure detailed in Saffe et al. (2015), which takes into account the individual and the mutual covariance terms of the error propagation. Within the errors, the parameters of the B star agree using the Sun or the A star as reference. We note that the A star is  $\sim 0.1$  dex more metal rich than the B star. Figure 1 shows abundance vs. excitation potential (top panel) and abundance vs.  $EW_r$  (bottom panel), both for the case (B–A).

<sup>3</sup> Echelle SpectroPolarimetric Device for the Observation of Stars.

<sup>4</sup> <http://www.gemini.edu/sciops/instruments/graces/spectroscopy/spectral-range-and-resolution>

<sup>5</sup> Open source Pipeline for ESPaDOnS Reduction and Analysis.

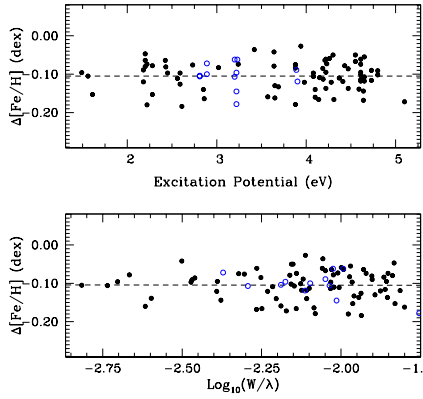
<sup>6</sup> <http://wiki.lna.br/wiki/espectro>

<sup>7</sup> We estimated a  $v_{\text{turb}}$  of  $0.91 \text{ km s}^{-1}$  for the Sun by requiring zero slope between Fe I abundances and  $EW_r$ .

<sup>2</sup> <http://exoplanet.eu/catalog/>

**Table 1.** Stellar parameters derived for each star.

(Star – reference)	$T_{\text{eff}}$ [K]	$\log g$ [dex]	[Fe/H] [dex]	$v_{\text{turb}}$ [km s <sup>-1</sup> ]
(A–Sun)	6036 ± 46	4.33 ± 0.13	0.277 ± 0.007	1.29 ± 0.07
(B–Sun)	6037 ± 37	4.38 ± 0.14	0.175 ± 0.006	1.21 ± 0.07
(B–A)	6035 ± 36	4.39 ± 0.10	-0.105 ± 0.006	1.22 ± 0.06


**Fig. 1.** Differential abundance vs. excitation potential (*upper panel*) and vs. reduced EW (*lower panel*) for the case (B–A). Filled and hollow circles correspond to Fe I and Fe II.

The next step was the derivation of abundances for all remaining chemical elements. The hyperfine structure splitting (HFS) was considered for VI, Mn I, Co I, Cu I, and Ba II using the HFS constants of Kurucz & Bell (1995) and performing spectral synthesis for these species. We also derived the Li I abundance using spectral synthesis with the resonance line 6707.80 Å, which includes the doublet 6707.76 Å, 6707.91 Å and HFS components. We corrected the Na I abundance for non-local thermodynamic equilibrium (NLTE) effects by interpolating in the data of Shi et al. (2004) and adopting Na(NLTE) – Na(LTE)  $\sim$  -0.07 dex for each star. We also applied NLTE corrections to O I (-0.18 dex and -0.17 dex for the A and B stars) by interpolating in the data of Ramírez et al. (2007). These corrections are relative to the Sun, which implies that NLTE effects for the case (B–A) are not significant given the high similarity between the stars A and B.

## 4. Results and discussion

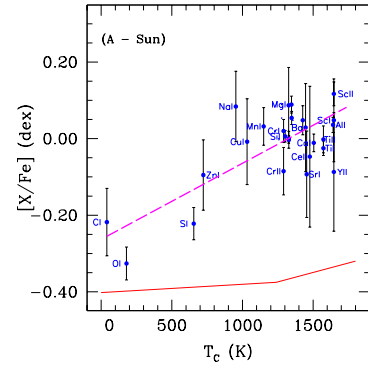
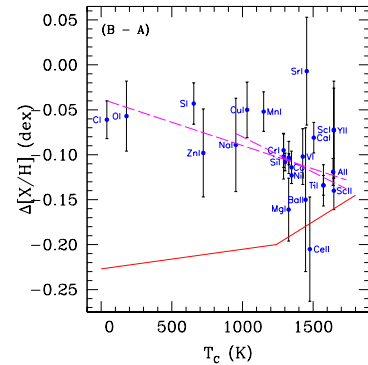
Condensation temperatures were taken from the 50%  $T_c$  values derived by Lodders (2003) for a solar system gas with [Fe/H] = 0. As suggested by the referee, it would be helpful to calculate other  $T_c$  sequences for different metallicity values. We corrected for GCE effects for the case (star – Sun), but not for the case (B–A) by adopting the GCE fitting trends of González Hernández et al. (2013), that is, we followed the same procedure as Saffe et al. (2015). Figure 2 presents the corrected abundance values vs.  $T_c$  for (A–Sun)<sup>8</sup>. Table 2 presents the slopes and uncertainties of the linear fits. The positive slopes for the case (star – Sun) indicate a higher content of refractories (those with  $T_c > 900$  K) relative to volatiles ( $T_c < 900$  K).

The differential abundances for (B–A) are presented in Fig. 3. The continuous line in this figure presents the solar-twins trend of Meléndez et al. (2009; vertically shifted). Long dashed

**Table 2.** Derived slopes (abundance vs.  $T_c$ ) and their uncertainties.

(Star – reference)	Slope $\pm \sigma$ [10 <sup>-5</sup> dex/K]	$V$ [mag]	Mass [ $M_{\odot}$ ]
(A–Sun)	+19.88 ± 2.29	$V_A = 11.12$	$M_A = 1.24 \pm 0.06$
(B–Sun)	+14.59 ± 1.93	$V_B = 11.38$	$M_B = 1.17 \pm 0.05$
(B–A)	-5.18 ± 1.15		
(B–A) <sub>Ref</sub>	-7.81 ± 2.61		

**Notes.** We also include the  $V$  magnitude and mass of the stars.


**Fig. 2.** Differential abundances vs.  $T_c$  for (A–Sun). The long dashed line is a weighted linear fit to the differential abundance values, while the continuous line shows the solar-twins trend of Meléndez et al. (2009).

**Fig. 3.** Differential abundances (B–A) vs.  $T_c$ . Long dashed lines are weighted linear fits to all species and to refractory species. The solar-twins trend of Meléndez et al. (2009) is shown with a continuous line.

lines are weighted linear fits to all elements and to refractory elements, showing similar negative slopes (see also Table 2). Some species such as Sr I and Ce II seem to possibly drive the trends, but we obtained very similar slopes after excluding these species. The average refractory and volatile [X/H] abundance values for (B–A) are  $-0.105 \pm 0.007$  dex and  $-0.065 \pm 0.015$  dex, which together with the negative slopes of Fig. 3 points toward a higher content of refractories in the A star than in its stellar companion.

### 4.1. Do the HAT-P-4 stars have a peculiar composition?

We detected a difference of  $\sim 0.1$  dex in metallicity between the stars A and B, which is one of the highest differences found in similar systems (e.g., Desidera et al. 2004, 2006). In this section we discuss the possible chemical pattern of the two stars.  $\lambda$  Boötis stars show moderate surface underabundances of most Fe-peak elements, but solar abundances of C, N, O, and S (e.g., Paunzen 2004), in contrast to the metal-rich content of stars A and B.

<sup>8</sup> For the B star, the values are similar to those of Fig. 2.

$\delta$  Scuti stars are pulsating variables with  $\sim$ A6-F6 spectral types and masses of between  $1.4\text{--}3.0 M_{\odot}$  (see, e.g., the catalogs of Rodríguez et al. 2000; Liakos & Niarchos 2017). We determined the stellar masses through a Bayesian method using the PARSEC<sup>9</sup> isochrones (Bressan et al. 2012), obtaining  $1.24 \pm 0.06 M_{\odot}$  and  $1.17 \pm 0.05 M_{\odot}$  for stars A and B. The temperature and mass of A and B are lower than those of all  $\delta$  Scuti stars of these catalogs. One of the coolest  $\delta$  Scuti stars with an abundance determination is CP Boo (6320 K, Galeev et al. 2012), which is  $\sim 300$  K hotter than the A star. However, the A star is enhanced ( $\geq 0.20$  dex) in Na I, Mg I, Al I, Sc II, V I, and strongly enhanced ( $> 0.40$  dex) in Sr II and Y II compared to CP Boo. Moreover, stars A and B lie beyond the instability strip boundaries (e.g., Figs. 6 and 7 of Liakos & Niarchos 2017), and no stellar pulsations have been reported.

Blue stragglers (BS) are stars that are significantly bluer than the main-sequence turnoff of the cluster (or population) to which they belong. There are binaries where one component is a BS, and it is impossible to fit both components with a single isochrone (Desidera et al. 2007). However, in our system the ages of the two stars agree within the errors ( $2.7 \pm 1.3$  Gyr and  $2.9 \pm 1.8$  Gyr), also when they are derived with the PARSEC isochrones (Bressan et al. 2012). BS stars present significant rotational velocities, intense activity, and very low Li content (e.g., Fuhrmann & Bernkopf 1999; Schirbel et al. 2015; Ryan et al. 2001). None of these characteristics are seen in star A or star B.

There are no firm reasons to identify any component of the binary system as peculiar. A possible different accretion would therefore be the most plausible explanation for the chemical differences observed. We estimated the rocky mass of depleted material in the A star following Chambers (2010). Adopting a convection zone similar to the current Sun ( $M_{cz} = 0.023 M_{\odot}$ ), we obtain  $M_{\text{rock}} \sim 10 M_{\oplus}$ . However, adopting a higher  $M_{cz}$  value (e.g.,  $0.050 M_{\odot}$ ) at the time of planet formation, we derive  $M_{\text{rock}} \sim 20 M_{\oplus}$ . Cody & Sasselov (2005) found that for stars with  $1.1 M_{\odot}$ , a polluted convection zone is slightly smaller ( $\sim 1\%$ ) than its unpolluted counterpart, but the trend is reversed for stars with  $M \leq M_{\odot}$ . More recently, Van Saders & Pinsonneault (2012) found that the acoustic depth to the base of the CZ varies at the  $0.5\text{--}1\%$  per 0.1 dex level in  $[Z/X]$ . A change of 1% in  $M_{cz}$  translates into  $\sim 0.5 M_{\oplus}$  of derived accreted material. Then, the estimate of at least  $10 M_{\oplus}$  of accreted material should be considered as a first-order approximation.

#### 4.2. Hot-Jupiter planet and the Li content

The formation of hot-Jupiter planets is mainly explained by the model of core accretion (Pollack et al. 1996) and by gravitational instability (Boss 2000). In both cases, some type of migration from the original location is required to explain the current orbit at  $\sim 0.04$  AU, with the possible accretion of inner planets into the star (e.g., Mustill et al. 2015). Another possibility is the in situ formation of the hot Jupiter (e.g., Bodenheimer et al. 2000), without migration from greater distances. However, the abundances of the C/O and O/H ratios suggest that some hot Jupiters originate beyond the snow line (Brewer et al. 2017). With the current data, it is difficult to distinguish between the different formation scenarios. Additional planets were searched for in the A star by transits (Smith et al. 2009; Ballard et al. 2011) and radial velocity (Knutson et al. 2014), without success. A scenario

<sup>9</sup> [http://stev.oapd.inaf.it/cgi-bin/param\\_1.3](http://stev.oapd.inaf.it/cgi-bin/param_1.3)

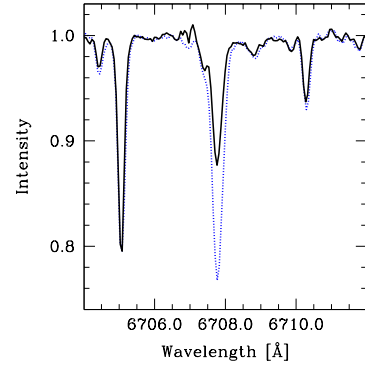


Fig. 4. Stellar spectra near the Li line 6707.8 Å for the A (blue dotted line) and B (black continuous line) stars.

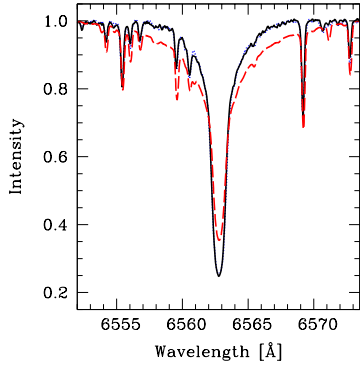
with a possible migration and accretion can therefore not be discarded.

Figure 4 shows that the line Li I 6707.8 Å is stronger in the A star (blue dotted line) than in the B star (black continuous line), with abundances of  $1.47 \pm 0.05$  and  $1.17 \pm 0.04$  dex. In this binary system, the star that hosts the planet also presents the higher Li content, in contrast to the model that explains the Li depletion by the presence of planets. A similar rotational velocity ( $7.0 \pm 0.9$  and  $6.1 \pm 1.0$  km s<sup>-1</sup> estimated from our spectra) suggests that the rotational mixing is not the cause of the different Li content. The slightly different masses of stars A and B suggest a difference of 0.2–0.3 dex in the Li abundances from fitting general literature trends (e.g., Fig. 3 of Delgado-Mena et al. 2015; and Fig. 9 of Ramírez et al. 2012). This can explain (at least in part) the higher Li content, in agreement with the scenario proposed by Ramírez et al. (2011) for 16 Cyg. Another possible scenario is the accretion of material in the A star, which could increase its Li abundance and agree with its higher metal content.

#### 4.3. Relative $T_{\text{eff}}$ difference

In this section we discuss the relative  $T_{\text{eff}}$  difference between stars A and B. Balmer lines could be used as  $T_{\text{eff}}$  proxies for solar-type stars (e.g., Barklem et al. 2002). Figure 5 presents the region near the H $\alpha$  line for the stars A (blue dotted line) and B (black continuous line) almost superimposed, together with a synthetic spectrum for comparison (red dashed line) calculated with  $T_{\text{eff}} = T_{\text{eff}}(\text{A}) - 150$  K = 5886 K. This suggests that stars A and B present a very similar  $T_{\text{eff}}$ . We also used the photometric calibration of Casagrande et al. (2010) with the colors  $(B - V)_T$  and  $(J - K_s)$  from the Tycho and 2MASS catalogs. We estimate a difference of +95 K and -5 K for (B-A). However, we note that the errors reported for  $V_T$  and  $B_T$  vary between 0.07–0.13 mag, while the errors in  $JHK$  are notably lower at 0.01–0.03 mag.

We also explored how the relative  $T_{\text{eff}}$  difference could change the abundance difference. For the case (B-A) we varied  $T_{\text{eff}}$  by -50, -100, and -150 K for the reference A star and recomputed new solutions for (B-A). In this way, we derived relative  $[\text{Fe}/\text{H}]$  differences between B and A of +0.11, +0.04, and -0.01 dex. This shows that a  $T_{\text{eff}}$  difference near  $\sim 150$  K would be required to remove the abundance offset between stars A and B. However, Fig. 5 shows that a synthetic spectra calculated for  $T_{\text{eff}} = T_{\text{eff}}(\text{A}) - 150$  K = 5886 K does not fit the observed H $\alpha$  profiles and does not respect the excitation and ionization equilibrium of the Fe lines (Fig. 6). We therefore find no clear reason to assume such a difference in  $T_{\text{eff}}$  between stars A and B.



**Fig. 5.** Spectral region near the H $\alpha$  line for stars A and B (blue dotted and black continuous line). A synthetic spectrum (red dashed line) with  $T_{\text{eff}}(\text{A})-150 \text{ K} = 5886 \text{ K}$  is also shown for comparison.

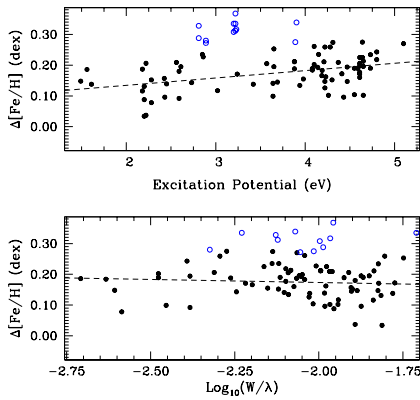


**Fig. 6.** Differential abundance vs. excitation potential (*upper panel*) and vs. reduced EW (*lower panel*) for the A star, adopting  $T_{\text{eff}}(\text{A})-150 \text{ K} = 5886 \text{ K}$ . Filled and empty circles correspond to Fe I and Fe II.

#### 4.4. Possible interpretations of the data

We propose that at the time of planet formation, the A star locked the orbiting refractory material in planetesimals and rocky planets, and formed the gas giant in the external disk. This was followed by the accretion of most of the refractories (possibly due to migration of the gas giant) onto the A star. This scenario explains the higher metallicity of the A star (no chemically peculiar patterns are seen), the higher refractory abundances, and the higher Li content. It is also supported by the slightly higher mass of the A star (corresponding to a lower convective mass and lower mixing of the accreted material) and by the non-detection of additional inner planets. A very similar scenario was recently proposed for the solar-twin star HIP 68468 (Meléndez et al. 2017), where the authors suggested that the possible inward migration of a close-in giant planet likely produces the engulfment of the inner planetary material by the star. This would explain the high Li content (0.6 dex greater than expected for its age), a refractory enhancement compared to the Sun, and a  $T_{\text{c}}$  trend. We also note that chemical tagging studies usually claim to be able to distinguish groups of stars with common origin within  $\sim 0.04$  dex of precision (e.g., Hogg et al. 2016). An intrinsic difference of  $\sim 0.1$  dex in metallicity would therefore imply a great challenge for these works.

*Acknowledgements.* The authors thank R. Kurucz and C. Sneden for making their codes available to us. E.J., R.P., M.F., and M.J.A. acknowledge the financial support from CONICET in the forms of Post-Doctoral Fellowships. We also

thank the referee Ivan Ramírez for constructive comments that greatly improved the paper.

## References

- Adibekyan, V., González Hernández, J., Delgado-Mena, E., et al. 2014, *A&A*, 564, A15
- Adibekyan, V., Delgado-Mena, E., Figueira, P., et al. 2016, *A&A*, 592, A87
- Ballard, S., Christiansen, J., Charbonneau, D., et al. 2011, *ApJ*, 732, 41
- Barklem, P. S., Stempels, H. C., Allende Prieto, C., et al. 2002, *A&A*, 385, 951
- Baumann, P., Ramírez, I., Meléndez, J., et al. 2010, *A&A*, 519, A87
- Bedell, M., Meléndez, J., Bean, J., et al. 2014, *AJ*, 795, 23
- Boss, A. 2000, *ApJ*, 536, 101
- Bodenheimer, P., Hubickyj, O., & Lissauer, J. 2000, *Icarus*, 143, 2
- Bressan, A., Marigo, P., Girardi, L., et al. 2012, *MNRAS*, 427, 127
- Brewer, J., Fischer, D., & Madhusudhan, N. 2017, *AJ*, 153, 83
- Carlos, M., Nissen, P., & Meléndez, M. 2016, *A&A*, 587, A100
- Casagrande, L., Ramírez, I., Meléndez, J., et al. 2010, *A&A*, 512, A54
- Chambers, J. 2010, *AJ*, 724, 92
- Cochran, W., Hatzes, A., Butler, P., & Marcy, G. 1997, *ApJ*, 483, 457
- Cody, A. M., & Sasselov, D. 2005, *AJ*, 622, 704
- Delgado-Mena, E., Israelian, G., González Hernández, J., et al. 2014, *A&A*, 562, A92
- Delgado-Mena, E., Bertan de Lis, S., Adibekyan, V., et al. 2015, *A&A*, 576, A69
- Desidera, S., Gratton, R. G., Scuderi, S., et al. 2004, *A&A*, 420, 683
- Desidera, S., Gratton, R. G., Lucatello, S., et al. 2006, *A&A*, 454, 581
- Desidera, S., Gratton, R. G., Lucatello, S., et al. 2007, *A&A*, 462, 1039
- Fuhrmann, K., & Bernkopf, J. 1999, *A&A*, 347, 897
- Galeev, A., Ivanova, D., Shimansky, V., et al. 2012, *Astron. Rep.*, 56, 11, 850
- Gonzalez, G. 1997, *MNRAS*, 285, 403
- Gonzalez, G. 2014, *MNRAS*, 441, 1201
- Gonzalez, G. 2015, *MNRAS*, 446, 1020
- González Hernández, J., Delgado-Mena, E., Sousa, S. G. et al. 2013, *A&A*, 552, A6
- Gratton, R. G., Bonanno, G., Claudi, R. U., et al. 2001, *A&A*, 377, 123
- Hogg, D., Casey, A., Ness, M., et al. 2016, *ApJ*, 833, 262
- Israelian, G., Santos, N., Mayor, M., et al. 2004, *A&A*, 414, 601
- Israelian, G., Delgado-Mena, E., Santos, N., et al. 2009, *Nature*, 462, 12
- King, J., Deliyannis, C., Hiltgen, D., et al. 1997, *AJ*, 113, 1871
- Kovács, G., Bakos, G., Torres, G., et al. 2007, *ApJ*, 670, L41
- Knutson, H., Fulton, B., Montet, B., et al. 2014, *ApJ*, 785, 126
- Kurucz, R. L. 1993, ATLAS9 Stellar Atmosphere Programs and 2 km s grid, Kurucz CD-ROM 13 (Cambridge, MA: Smithsonian Astrophysical Obs.)
- Kurucz, R., & Bell, B. 1995, Atomic Line Data, Kurucz CD-ROM, 23, (Cambridge, MA: Smithsonian Astrophysical Obs.)
- Laws, C., & Gonzalez, G. 2001, *ApJ*, 553, 405
- Liakos, A., & Niarchos, P. 2017, *MNRAS*, 465, 1181
- Liu, F., Asplund, M., Ramírez, I., et al. 2014, *MNRAS*, 442, L51
- Lodders, K. 2003, *AJ*, 591, 1220
- Luck, R., & Heiter, U. 2006, *AJ*, 131, 3069
- Mack, C., Schuler, S., Stassun, K., et al. 2014, *ApJ*, 787, 98
- Martoli, E., Teeple, D., Manset, N., et al. 2012, *Software and Cyberinfrastructure for Astronomy II, Proc. SPIE*, 8451, 21
- Meléndez, J., Asplund, M., Gustafsson, B., et al. 2009, *AJ*, 704, L66
- Meléndez, J., Ramírez, I., Karakas, A., et al. 2014, *AJ*, 791, 14
- Meléndez, J., Bedell, M., Bean, J., et al. 2017, *A&A*, 597, A34
- Mugrauer, M., Ginski, C., & Seeliger, M. 2014, *MNRAS*, 439, 1063
- Mustill, A., Davies, M., & Johansen, A. 2015, *ApJ*, 808, 14
- Pauzen, E. 2004, The A-Star Puzzle, eds. J. Zverko, J. Ziznovsky, S. Adelman, & W. Weiss (Cambridge Univ. Press), *IAU Symp.*, 224, 443
- Pollack, J., Hubickyj, O., Bodenheimer, P., et al. 1996, *Icarus*, 124, 62
- Ramírez, I., Allende Prieto, C., & Lambert, D. 2007, *A&A*, 465, 271
- Ramírez, I., Meléndez, J., & Asplund, M. 2009, *A&A*, 508, L17
- Ramírez, I., Meléndez, J., Cornejo, D., et al. 2011, *ApJ*, 740, 76
- Ramírez, I., Fish, J., Lambert, D., et al. 2012, *ApJ*, 756, 46
- Rodríguez, E., López-González, M., & López de Coca, P. 2000, *A&AS*, 144, 469
- Ryan, S., Beers, T., Kajino, T., & Rosolankova, K. 2001, *AJ*, 547, 231
- Saffe, C. 2011, *RMxAA*, 47, 3
- Saffe, C., Flores, M., & Buccino, A. 2015, *A&A*, 582, A17
- Saffe, C., Flores, M., Jaque Arancibia, M., et al. 2016, *A&A*, 588, A81
- Schirbel, L., Meléndez, J., Karakas, A., et al. 2015, *A&A*, 584, A116
- Shi, J. R., Gehren, T., & Zhao, G. 2004, *A&A*, 423, 683
- Schuler, S., Cunha, K., Smith, V., et al. 2011, *ApJ*, 737, L32
- Smith, V., Cunha, K., & Lazzaro, D. 2001, *AJ*, 121, 3207
- Smith, A. M., Hebb, L., Collier Cameron, A., et al. 2009, *MNRAS*, 398, 1827
- Sneden, C. 1973, *ApJ*, 184, 839
- Tucci Maia, M., Meléndez, J., & Ramírez, I. 2014, *ApJ*, 790, L25
- Van Saders, J., & Pinsonneault, M. 2012, *AJ*, 746, 16